Simultaneous mooring-based measurements of seawater CO_2 and O_2 off Cape Hatteras, North Carolina

M. D. DeGrandpre[1] and T. R. Hammar

Department of Marine Chemistry and Geochemistry, Woods Hole Oceanographic Institution, Woods Hole, Massachusetts 02543

D. W. R. Wallace and C. D. Wirick

Oceanographic and Atmospheric Sciences Division, Department of Applied Science, Brookhaven National Laboratory, Upton, New York 11973

Abstract

We deployed CO_2 and O_2 sensors on the U.S. continental shelf off Cape Hatteras, North Carolina, during late summer 1994. A continuous 32-d gas record was obtained at 20 m in 25 m of water, below the thermocline for most of the period. Analysis of the correlation between CO_2 and O_2 indicates that biological and advective processes dominated the gas variability, with small or insignificant fluxes due to air–sea exchange, vertical eddy diffusion, and carbonate dissolution or formation. The observed O_2:CO_2 correlation was 1.39, within the range predicted for the photosynthetic quotient. Photosynthesis and respiration appeared to be tightly coupled, resulting in no net community production in these waters during the late summer. It is evident from these results that the combination of mooring-based CO_2 and O_2 measurements will be a powerful tool for studying the marine carbon cycle.

The ability to predict future levels of atmospheric CO_2 under different energy use and climate change scenarios is dependent on our understanding of the processes that control the partial pressure of CO_2 (pCO_2) in surface ocean waters. Ocean pCO_2 has large temporal and spatial variability, which has been difficult to characterize from ships (e.g. Watson et al. 1991; Bates et al. 1996). Physical and biological oceanographers often rely upon moored instrumentation for studying complex ocean processes (e.g. Dickey et al. 1993). Unfortunately, most parameters of biogeochemical interest are not readily measured on moorings. However, recent technological breakthroughs have made it possible to measure seawater pCO_2 on moorings (DeGrandpre 1993; DeGrandpre et al. 1995a; Friederich et al. 1995). In this study we have used our Submersible Autonomous Moored Instruments for seawater CO_2 (DeGrandpre 1993; DeGrandpre et al. 1995a), also known as SAMI-CO_2, to measure ocean pCO_2. We have combined the SAMI-CO_2s with commercially available O_2 electrodes to record the first simultaneous time series of CO_2 and O_2 on an ocean mooring. The instruments were deployed on the U.S. Middle Atlantic Bight (MAB) ~16 km off Cape Hatteras, North Carolina. Shelf water is thought to flow off the Cape Hatteras shelf into the North Atlantic (Biscaye et al. 1994), possibly exporting significant amounts of carbon (in various forms) to the interior ocean (Blair et al. 1995).

Therefore, the focus of this study was to determine CO_2 sources and sinks within MAB waters prior to movement of the water off the shelf. An important additional objective was to provide a rigorous field test of the moored instrumentation.

The field study consisted of a 46-d deployment in 25 m of water beginning in late July 1994. SAMI-CO_2s were moored at 5 and 20 m and each was accompanied by two O_2 sensors. The sensor depths were chosen so that the sensors would reside within the surface and bottom mixed layers. We obtained 3-d and 32-d time series from the 5-m and 20-m SAMI-CO_2s, respectively. Because the time series from 5-m depth was abbreviated owing to damage of the reagent bags by wave action, only the 32-d time-series from the 20-m SAMI-CO_2 and O_2 sensors is presented here. Analysis of the O_2:CO_2 correlation at 20 m indicates that biological and advective processes dominated the gas variability, with small or insignificant fluxes due to air–sea exchange, vertical eddy diffusion, and carbonate dissolution or formation. The observed O_2:CO_2 ratio was 1.39, within the range predicted for the photosynthetic quotient (PQ). Photosynthesis and respiration seemed to be tightly coupled, resulting in no net community production in these waters during the late summer.

Methods

Detailed discussions of the SAMI-CO_2 operating principle are given by DeGrandpre (1993) and DeGrandpre et al. (1995a). Briefly, the instrument operates by measuring the optical absorbance of a pH indicator solution that is equilibrated with seawater pCO_2 via a gas-permeable membrane. During each measurement cycle, new indicator solution is pumped into a 50-μl tubular silicone rubber membrane, pushing the CO_2-equilibrated solution into a low-volume fi-

---

ber optic flow cell where the solution absorbance is recorded at three wavelengths. We have achieved nearly drift-free operation for month-long periods by flushing out the pH indicator for each measurement and by using ratios of indicator optical absorbances. Calibrations are performed in a temperature-controlled ($\pm 0.02°C$) water-filled chamber. CO_2 calibration gases are generated by diluting a 1,600 ppm CO_2 (in air) standard with nitrogen by means of two mass flow controllers. During the calibration, gas concentrations are monitored with an infrared CO_2 analyzer (LI-6251, LiCor, Inc.) calibrated with accurately known (± 1 ppm) CO_2 gas standards. Calibrations are performed at the expected seawater temperature and data are later corrected for differences between the calibration and measurement water temperature. The temperature coefficient of the response, determined by varying the equilibration temperature, is ~ 7 μatm $°C^{-1}$. Measurement precision and accuracy estimated from the calibration are approximately ± 1 μatm and ± 2 μatm, respectively.

O_2 measurements were made with pulsed polarographic electrodes (model 6000, Endeco YSI, Inc.), which also recorded depth, temperature ($\pm 0.1°C$), and salinity ($\pm 0.1‰$). The O_2 sensors are calibrated with water-saturated air and measurements are compared to Winkler titrations prior to deployment, generally agreeing to $\pm 0.5\%$ saturation. The instrument calibrations were checked upon retrieval and indicated $\sim 1\%$ drift from the original calibration. This observation is also supported by the in situ O_2 replicates, which agreed to $\pm 1.5\%$ O_2 saturation. CO_2 and O_2 were measured every half-hour for a total of $\sim 1,540$ measurements during the 32-d period.

Other field data were available for interpretation of the in situ gas data. These included data from a thermistor chain that was placed between the 5-m and 20-m sensors with thermistors located at 8, 11, 14, and 17 m. Measurements of wind (direction and magnitude) and wave (height and period) parameters were available from a nearby NOAA meteorological buoy. Surface currents and depth-resolved salinity (2, 8, 13, and 24 m) were also measured on a nearby mooring starting on 7 August 1994 (S. Lentz pers. comm.).

Results and discussion

The 32-d time series obtained from the 20-m SAMI-CO_2 and O_2 sensors are shown in Fig. 1. The pCO_2 and O_2 levels fall within the range measured by us (D. Wallace unpubl. results) and others (Sharp and Church 1981; C. Reimers pers. comm.) for subpycnocline waters on the MAB. The striking inverse relationship in Fig. 1 suggests that CO_2 and O_2 were controlled by the same processes in the MAB bottom water and also suggests that neither measurement had significant long-term drift during the 32-d period. In our discussion we first address the general qualitative features of the gas time series and then present a more detailed analysis of the $CO_2 : O_2$ correlation by use of a one-dimensional mixing model.

Gas time series—Many of the rapid short-term changes in pCO_2 and O_2 seem to be related to advective processes in the water column. Water-column isotherms (Fig. 1C) esti-

mated from the thermistor chain data show that the water column was stratified by a strong thermocline for the entire period. Mixed-layer depths ranged from 6 to 12 m, typical of late summer on the MAB (Falkowski et al. 1983). The temperature record also shows that the water column around 20 m was often not well mixed (Fig. 1C). The displacement of isotherms at 20 m was frequently coincident with rapid changes in CO_2 and O_2. For example, in Fig. 1, gas fluctuations during year-days 203–207 (23–27 July) were followed by a more quiescent period (year-days 207–211, 27–31 July) during which the bottom water evolved from poorly mixed to well-mixed states (Fig. 1C,D). Evidently, concentration gradients within the thermocline gave rise to these short-term fluctuations. Comparison of the depth (not shown) and temperature records shows that the thermocline depth changed with the tidal cycle. Therefore, much of the noisy appearance of the gas time series can be attributed to tidal oscillations that raise or lower the thermocline depth.

Although the short-term (<1 d) changes were at times large, they remained centered around a similar baseline until around day 224 (13 August) when the pCO_2 rose and O_2 dropped for an extended period. This deviation does not seem to correspond to any distinct hydrographic or meteorological events such as advection of different water masses, cloud cover, or changes in winds or waves. Work by others on the New York Bight (Falkowski et al. 1980) demonstrated that oxygen depletion can occur during upwelling events that erode the bottom-water volume, reducing its capacity to oxidize organic material below the pycnocline. Falkowski et al. (1980) also showed that phytoplankton can concentrate below the summer pycnocline and increase the oxygen demand of the bottom water. We do not have broadscale hydrographic data and chlorophyll fluorescence or other means for estimating biomass at the 20-m site in order to determine if upwelling or increased respiration led to the O_2 decline on day 224.

$pCO_2 : O_2$ *correlation*—The pCO_2 and O_2 had a consistent correlation ($r^2 = -0.973$) (Fig. 2) for the entire 32 d. Neither correlated significantly with temperature or salinity (shown for pCO_2 only in Fig. 2). Many physical (mixing and advection, warming and cooling, gas exchange), biological (photosynthesis, respiration), and chemical (carbonate formation and dissolution, photooxidation) processes can contribute to the pCO_2 and O_2 variability in the euphotic zone, and the relationship of pCO_2 and O_2 will depend on their relative contributions. Others (Simpson 1985; Hoppema 1991; Taylor et al. 1992) have found considerable scatter and nonlinear relationships between pCO_2 and O_2 % saturation. Despite the potential complexity of these two gases, our time-series data show a remarkably tight $CO_2 : O_2$ relationship, suggesting that the 20-m sensors were exposed to water with a similar physical and biogeochemical history. We first assess contributions from physical processes.

Advective events—The salinity data in Fig. 1D show that high salinity water was present at the 20-m isobath during most of the period. The *T-S* correlation (Fig. 3) suggests that the water originated from the continental slope (Churchill et al. 1993). A brief deviation occurred on 6 August
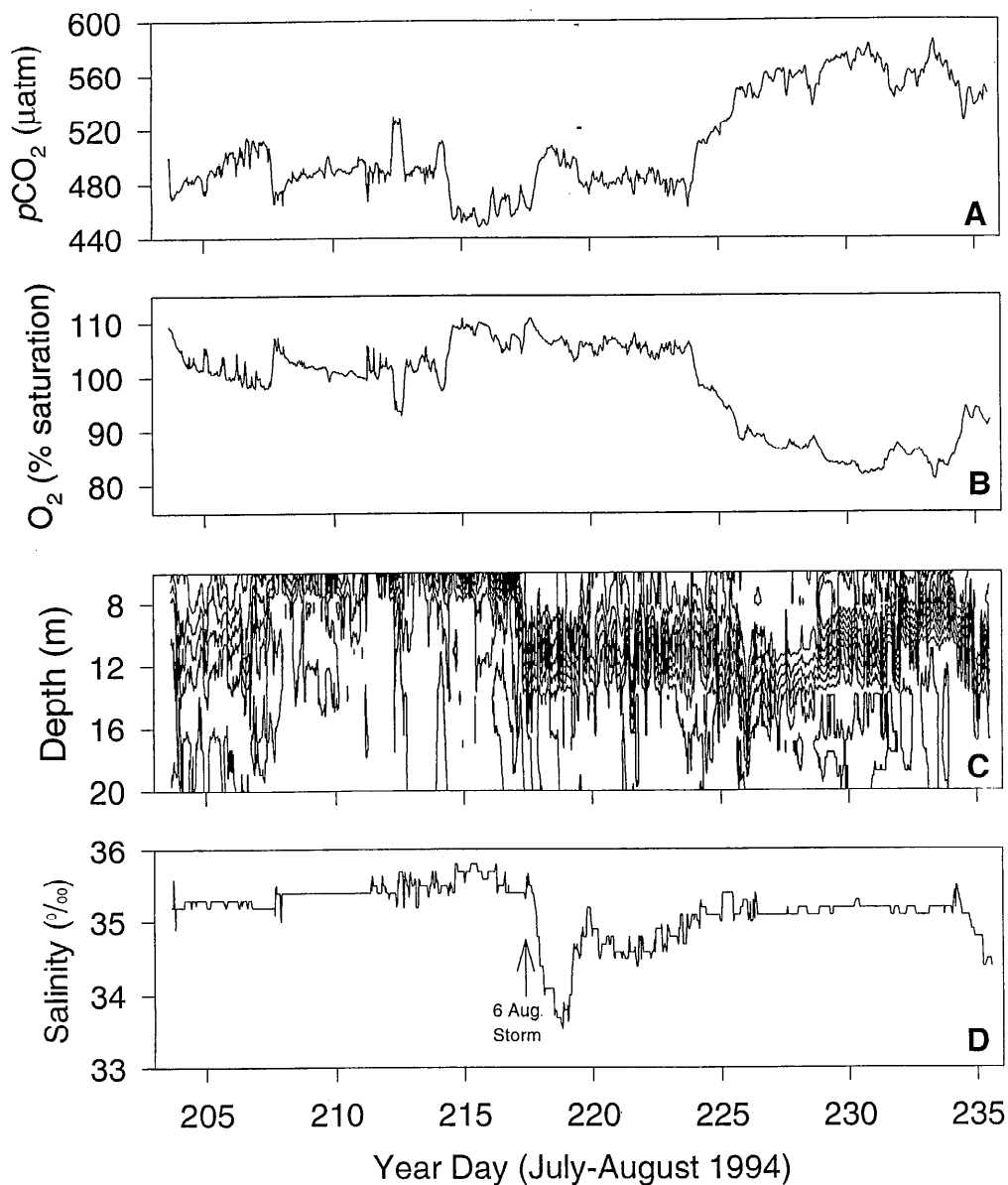
Fig. 1. A,B. Time-series of pCO$_2$ and O$_2$ from the Cape Hatteras mooring deployment starting 23 July 1994. The sensors were moored at 20 m on the 25-m isobath. C. Temperature isotherms calculated from thermistor chain data collected at the same location. The 1°C contours from 13 to 25°C are shown. D. Salinity (±0.1‰) measured by the Endeco model 6000.

(year-day 217) when a storm brought lower salinity water into the area (Fig. 1D). This lower salinity shelflike water had a different $CO_2 : O_2$ signature (higher pCO$_2$, lower O$_2$), as indicated by the circled points in Fig. 4. From this observation it is feasible that if other water masses were periodically advected into the area, such as Chesapeake Bay or Gulf Stream waters, they would appear as a different $CO_2 : O_2$ correlation in Fig. 4. As a result, the tight $CO_2 : O_2$ correlation supports that lateral advection of widely different water masses was not a major source of gas variability.

Vertical mixing of the water column must also be considered. The surface salinity and O$_2$ records showed that surface salinities were 1–4‰ lower than at 20 m; surface and 20-m O$_2$ concentrations differed by <7%. The pCO$_2$ measured by SAMI-CO$_2$ at 5 m during the first 3 d of the deployment ranged from 290 to 310 μatm and had risen to atmospheric equilibrium (360 μatm) by early September based upon shipboard measurements, when the mooring was retrieved. Mixing of the low pCO$_2$ surface water into the bottom water would have appeared as a large deviation from the correlation in Fig. 4. As stated before, the 6 August storm brought in water with a different pCO$_2 : O_2$ signature but not a surface signature, i.e. lower pCO$_2$. The consistently high salinity at 20 m also suggests that the sensors were isolated from the surface water.
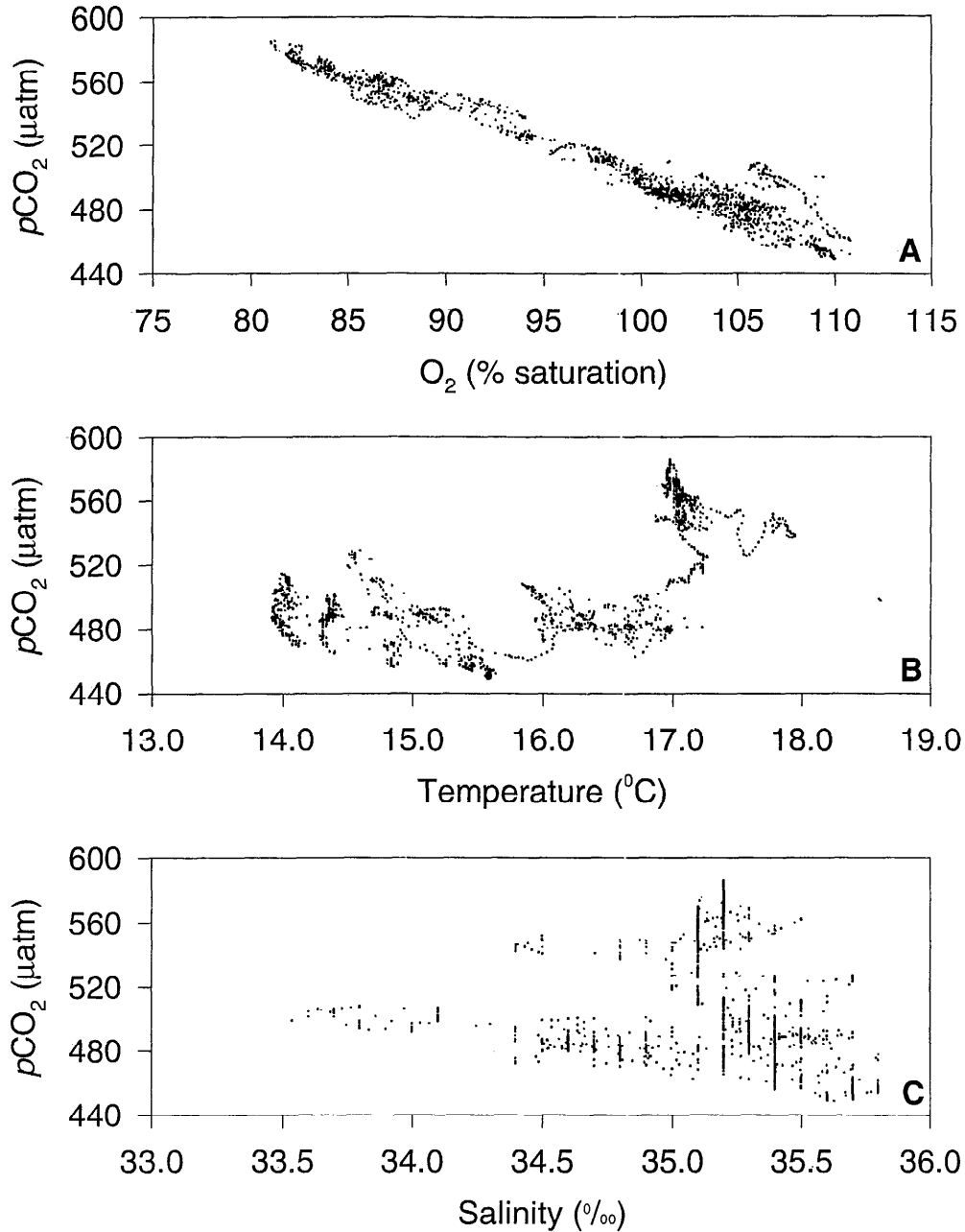
Fig. 2.   A. pCO_2 vs. O_2 time-series data from Fig. 1. B. pCO_2 vs. the in situ temperature measured by the SAMI-CO_2. C. pCO_2 vs. salinity from Fig. 1.

Air–sea exchange and eddy diffusion—Other physical processes such as gas exchange and turbulent (eddy) diffusion act to restore gas concentrations to atmospheric equilibrium. We evaluated the CO_2:O_2 correlations that would result from gas exchange and eddy diffusion by using a simple one-dimensional mixing model. We discuss the slope of the CO_2:O_2 correlation to assess contributions from different processes rather than attempt quantitative estimates of gas variability with our limited spatial resolution. Gas exchange was calculated by means of

$$H_s \frac{dC_s}{dt} = K_T S \Delta C. \qquad (1)$$

H_s is the mixed-layer depth (10 m), C_s is the estimated water column concentration, ΔC is the partial pressure difference (CO_2 or O_2) across the air–sea interface, S is the gas solubility, and K_T is the gas transfer coefficient. The K_T for CO_2 was calculated from wind speed (Liss and Merlivat 1986) assuming an average wind speed of 5 m s^{-1}. The K_T was corrected for O_2 with the O_2 diffusion coefficient. Because of the redistribution of CO_2 through the carbonate equilibria, the total CO_2 (TCO$_2$, the sum of CO_2, HCO$_3^-$, and CO$_3^{2-}$) must be used for C_s. The initial TCO$_2$ was set at 2,120 μmol kg^{-1}, estimated by means of a salinity–alkalinity relationship described in more detail below. Gas solubilities and equilib-
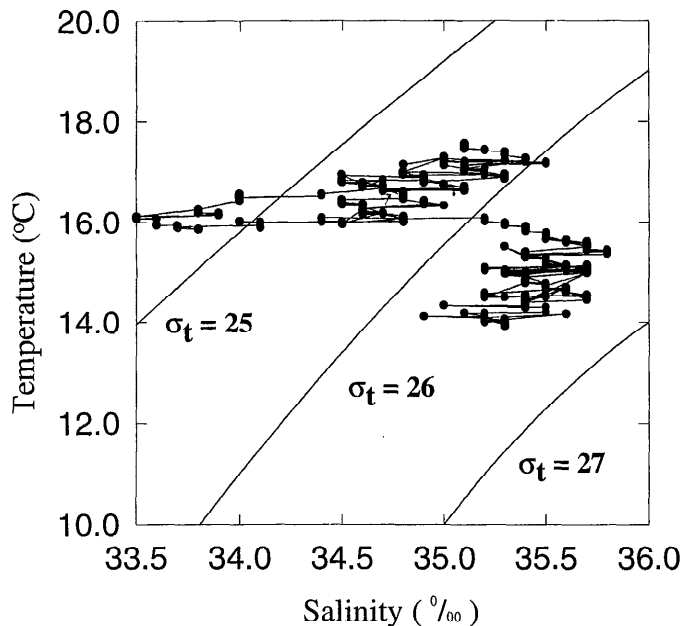
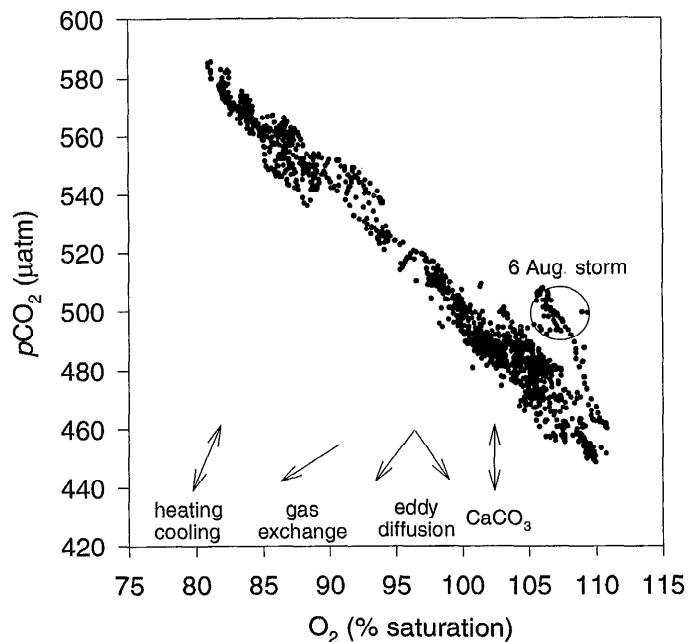Fig. 3. *T-S* diagram from the 20-m temperature and salinity data.

Fig. 4. pCO_2 vs. O_2 time-series data from Fig. 1. Arrows depict the expected directions of variability owing to different physical and biogeochemical forcings (*see text*).

rium constants were calculated with the salinity and temperature data in Fig. 1 (Millero et al. 1993; Lewis and Wallace 1995; Forstner and Gnaiger 1983).

The expected direction of variability due to air–sea exchange assuming O_2 is >100% saturation is depicted by an arrow in Fig. 4. Although CO_2 and O_2 exchange rates are very similar (e.g. DeGrandpre et al. 1995*b*), the rate of change of pCO_2 is reduced relative to O_2 because of buffering through the carbonate equilibria. Therefore, the shallow slope of the arrow reflects the higher rate of change of O_2 relative to pCO_2. If air–sea exchange were a dominant mechanism in regulating the CO_2:O_2 relationship, one would expect variability along this axis (when O_2 was above saturation). The measured correlation (Fig. 4) is nearly orthogonal to the air–sea exchange direction, providing evidence that gas exchange was not a major influence.

Vertical eddy diffusion will also result in CO_2 and O_2 fluxes into or out of the bottom water. Variability owing to this flux can be estimated from

$$H_b \frac{dC_b}{dt} = \frac{K_z}{H_t}(C_s - C_b). \qquad (2)$$

H_b is the bottom water depth (10 m), H_t is the thermocline depth (5 m), C_s is the surface mixed-layer concentration (which is assumed not to be affected by gas exchange because surface pCO_2 was near atmospheric equilibrium), C_b is the bottom water concentration, and K_z is the vertical eddy diffusivity. K_z was set equal to 0.1 cm^2 s^{-1} determined from previous work on the MAB (Wallace 1994). TCO_2 was used as the "diffusing species" and the initial conditions were set equal to 1,910 and 2,120 μmol kg^{-1} in the surface and bottom water, respectively. The surface and bottom water O_2 time-series records show that the surface O_2 was typically, but not always, higher than the bottom-water O_2. Fluxes

could therefore be either out of or into the bottom water during different periods. Use of Eq. 2 with different bottom and surface O_2 levels results in a wide range of CO_2:O_2 relationships (Fig. 4), with variability possibly lying along the observed correlation.

In addition to air–sea exchange and eddy diffusion, heating and cooling will also affect gas levels relative to atmospheric saturation. The direction of variability expected due to temperature changes is indicated in Fig. 4. Increasing temperatures, which will increase pCO_2 and O_2 % saturation, are indicated by the upward-pointing arrow.

Note that, although not common in MAB waters, carbonate formation and dissolution is another potential source of variability, and would act to alter pCO_2 via the reaction

$$Ca^{2+} + 2HCO_3^- \rightleftharpoons CaCO_3 + CO_2 + H_2O. \qquad (3)$$
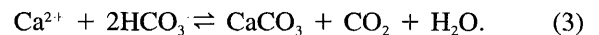
The CO_2 would change independently of O_2, as shown in Fig. 4, if this reaction were a significant source of variability.

Biological contributions—The variability of CO_2 and O_2 due to photosynthesis and respiration may be assessed by examining the relationship between TCO_2 and O_2. Although TCO_2 was not directly measured, it can be calculated for the 32-d time series by using the combination of pCO_2 and alkalinity (Millero et al. 1993) and assuming that alkalinity is linearly related to salinity. We have found from our field measurements that alkalinity on the MAB can be determined to ±20 μmol kg^{-1} by using alkalinity = 669.9 + (46.44 × salinity). The alkalinity uncertainty results in a ±18 μmol kg^{-1} uncertainty in the calculated TCO_2. The calculated TCO_2 ranged between 2,050 and 2,150 μmol kg^{-1}, which is within the range measured by others (Sharp and Church
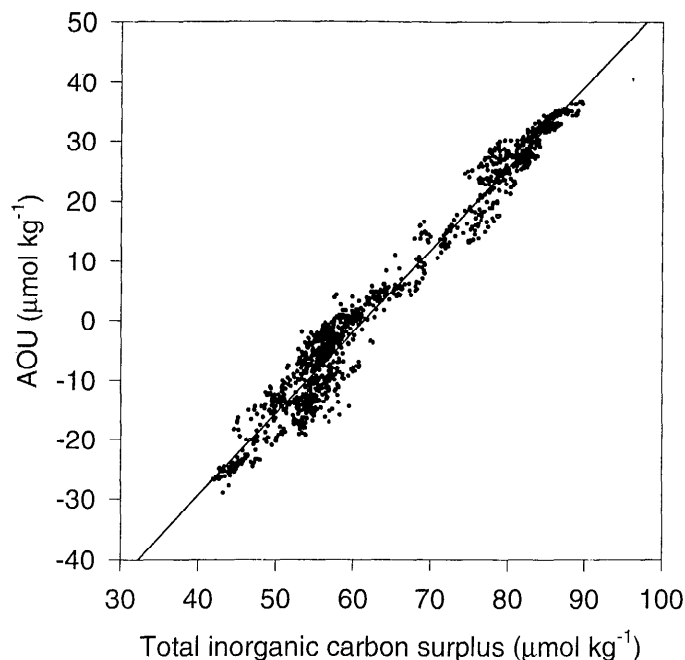
Fig. 5.   The apparent O_2 utilization (AOU) vs. the total inorganic carbon surplus. TCO_2 was calculated as described in the text. Both AOU and surplus TCO_2 were calculated relative to atmospheric saturation (pCO_2 was set at 360 μatm for TCO_2) by using the in situ temperature and salinity (Fig. 1). The least-squares regression line is shown (r^2=0.966). The slope of the line is equal to 1.39±0.02 mol O_2 (mol CO_2)$^{-1}$.

1981; C. Reimers pers. comm.) for bottom waters on the MAB.

To determine the stoichiometric relationship between CO_2 and O_2, the apparent O_2 utilization (AOU) is plotted in Fig. 5 vs. the surplus TCO_2 calculated relative to atmospheric saturation at 360 μatm. The data collected during the 6 August storm were omitted to reduce the influence of different water masses on the TCO_2 : AOU correlation. Typical marine biological production has a PQ (mol O_2 produced per mol CO_2 consumed) between 1.0 and 1.4 (Williams and Robertson 1991; Laws 1991). The equation for the line in Fig. 5 was obtained as the geometric mean regression according to the method proposed by Ricker (1973). The resulting slope is 1.39±0.02 mol O_2 (mol CO_2)$^{-1}$, falling within the range that would be expected for biological production. Separating the night and day data and performing the same calculations indicated that there are no significant differences in the TCO_2 : AOU relationship between night and day. Sharp and Church (1981) found a tight correlation (r^2 = 0.94) between TCO_2 and AOU in MAB bottom water, although their estimated PQ was 1.27 mol O_2 (mol CO_2)$^{-1}$. Undoubtedly the physical processes that we have discussed would have some effect on the TCO_2 : AOU relationship, although the high degree of linearity and the correspondence with the predicted PQ suggests that their contributions were minimal.

Our field-estimated PQ of 1.39 represents an average PQ for a 32-d period. Other estimates of PQ have been based on short-term incubations in which production of O_2 and

uptake of ^{14}C were measured. This approach has resulted in a large range of estimated PQs (0.5–3.5) (Williams and Robertson 1991). Our estimate falls within the range expected for the production of photosynthetic carbon and supports the contention by others (Williams and Robertson 1991; Laws 1991) that high PQs result from systematic differences between the O_2 and ^{14}C methods.

In situ estimates of production—Water column measurements of O_2 and CO_2 can also be used to estimate rates of production and consumption of photosynthetic carbon (K. M. Johnson et al. 1979; K. S. Johnson et al. 1981; Oudot 1989; Robertson et al. 1993; Chipman et al. 1993). In such studies, the rates of change of either TCO_2 or O_2 were measured within the surface mixed layer to estimate production. Our TCO_2 and O_2 rates can be directly compared to each other by converting the O_2 data to CO_2 assuming a PQ of 1.39. Both the TCO_2 and O_2 data were low-pass-filtered with a 12-h cutoff to reduce contributions from short-term advection. Figure 6 shows the rates of change of carbon by using the low-pass-filtered TCO_2 and O_2 data. The CO_2 and O_2 estimated rates are very similar except during the storm on 6 August. The lower salinity water advected in during that period reduced the calculated alkalinity and, as a result, changed the TCO_2. The rates of change were highly variable, although daytime maxima and nighttime minima are clearly evident. Average peak daytime and nighttime rates and their corresponding average peak times are shown in Table 1.

Peak carbon production (uptake of CO_2) occurred in the afternoon on average (Table 1), as would be expected from phytoplankton photosynthesis. Light attenuation measurements on the MAB shelf indicate a typical attenuation of 0.1 m^{-1} during August (DeGrandpre et al. 1996). Therefore, ~14% of the incident radiation would be present at 20 m, which could support significant production. The amplitude variability, however, does not correlate with solar insolation measured on a nearby meteorological buoy. The variability must be attributed to some other physical or biogeochemical forcing. As discussed earlier, it seems that CO_2 and O_2 concentration gradients existed within the bottom water. Others have shown that the chlorophyll maximum and nutricline are often located below the late summer thermocline on the MAB (Falkowski et al. 1983; Sharp and Church 1981), indicating that photosynthesis is fast relative to mixing processes in the bottom water. In this situation, the rates of change recorded at 20 m could be influenced by changes in the sensor locations relative to the chlorophyll maximum; that is, the resulting bottom-water concentration gradients could generate a periodic cycle if the gradients were shifting with periodic forcings such as tides or solar heating.

As we discussed earlier, changes in CO_2 and O_2 often followed the tidal cycle. This periodic advective cycle clearly contributed to the variability in peak amplitude and time (Table 1). Additionally, diurnal convection that occurs from heating and cooling can alter gas concentrations and shift the peak production off of peak daylight periods (McNeil and Farmer 1995). Contributions from diurnal convection were difficult to assess from the temperature data because of the large tidal contribution. It is therefore evident that because of the complex stratification during this period, a
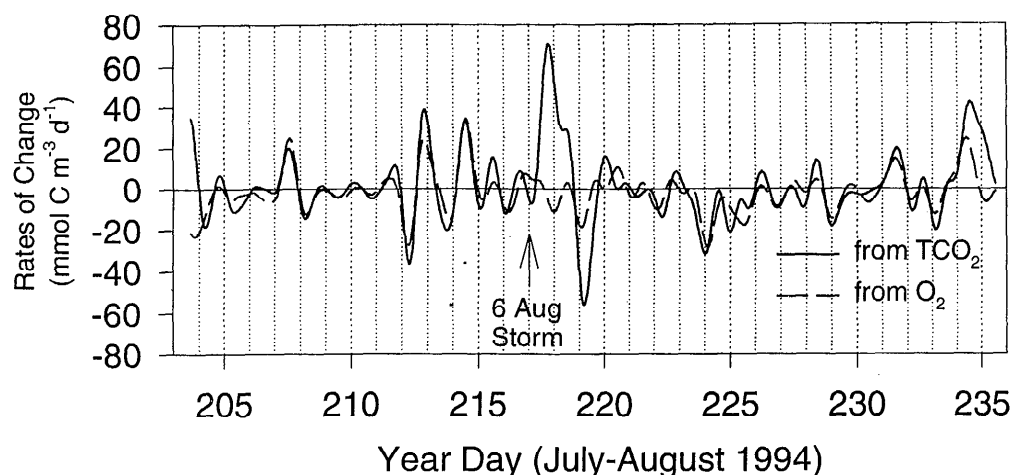
Fig. 6. Rates of change of TCO$_2$ and O$_2$ in terms of photosynthetic carbon calculated from the TCO$_2$ and O$_2$ data. O$_2$ data were converted to mmol C m^{-3} d^{-1} by using 1.39 mol O$_2$ (mol CO$_2$)$^{-1}$. All data were low-pass-filtered with a 12-h cutoff.

single-point measurement may not accurately estimate daily total production within the bottom water.

Average rates of change over the entire 32-d period were -1.2 mmol C m^{-3} d^{-1} and $+1.5$ mmol C m^{-3} d^{-1} as estimated from the CO$_2$ and O$_2$ data, respectively. These values are very small relative to the average daily peaks (Table 1). Although the daily rates do not represent an integrated production, it is possible that the long-term data average out the advective fluctuations, giving an estimate of net production in the bottom water during the 32-d period. This argument is particularly compelling since the very low values support other evidence that primary production and respiration are tightly coupled on the MAB shelf during late summer, resulting in no significant net production (Falkowski et al. 1983).

Conclusion

Through analysis of the correlation between CO$_2$ and O$_2$ we have shown that biological production and respiration controlled the relationship of these gases. Most of the large, rapid changes evident in the time series have been attributed to shifting concentration gradients. The concentration gradients are established by phytoplankton gradients within the water column and, hence, the shifting gradients reflect the biological imprint. A single gas time series of either CO$_2$ or O$_2$ would cause the researcher to speculate on possible bi-

ological contributions. We have shown that the combination of pCO$_2$ and O$_2$ is a powerful tool for determining the sources of gas variability in a marine ecosystem. In this study the interpretation was simplified because of the presence of a relatively consistent water mass that was isolated from the surface. In future studies, pCO$_2$ and O$_2$ may be acted upon by other physical forcings such as air–sea exchange that will change the relationship shown in Fig. 4. By combining our CO$_2$ and O$_2$ measurements with time-series measurements of inert gases, such as N$_2$ (Farmer et al. 1993), it may be possible to separate physical and biological contributions to gas variability. The air–sea flux may then be estimated by means of conventional gas transfer models based on wind speed (Liss and Merlivat 1986) or others incorporating wave and bubble models (Wallace and Wirick 1992; Farmer et al. 1993). Such studies will lead to a better understanding of the mechanisms for gas exchange across the air–sea interface.

References

BATES, N. R., A. F. MICHAELS, and A. H. KNAP. 1996. Seasonal and interannual variability of oceanic carbon dioxide species at the U.S. JGOFS Bermuda Atlantic Time-series Study (BATS) site. Deep-Sea Res. Part 2 **43:** 347–383.

BISCAYE, P. E., C. N. FLAGG, AND P. G. FALKOWSKI. 1994. The shelf edge exchange processes experiment, SEEP-II: An introduction to hypotheses, results and conclusions. Deep-Sea Res. Part 2 **41:** 231–252.

BLAIR, N. E., G. R. PLAIA, S. E. BOEHME, D. J. DEMASTER, AND L. A. LEVIN. 1995. The remineralization of organic carbon on the North Carolina continental slope. Deep-Sea Res. Part 2 **41:** 755–766.

CHIPMAN, D. W., J. MARRA, AND T. TAKAHASHI. 1993. Primary production at 47°N and 20°W in the North Atlantic Ocean: A comparison between the ^{14}C incubation method and the mixed layer carbon budget. Deep-Sea Res. Part 2 **40:** 151–169.

CHURCHILL, J. H., E. R. LEVINE, D. N. CONNORS, AND P. C. CORNILLON. 1993. Mixing of shelf, slope and Gulf Stream water over the continental slope of the Middle Atlantic Bight. Deep-Sea Res. **40:** 1063–1085.

Table 1. Average peak rates of change of O$_2$ and TCO$_2$ in terms of photosynthetic carbon and corresponding peak times. Times are reported as EST.

	Night rates (mmol C m^{-3} d^{-1})	Peak time	Day rates (mmol C m^{-3} d^{-1})	Peak time
From O$_2$	10±8	0214(±5.0 h)	7±10	1330(±4.8 h)
From CO$_2$	12±12	0305(±5.3 h)	12±13	1355(±5.6 h)

DEGRANDPRE, M. D. 1993. Measurement of seawater pCO_2 using a renewable-reagent fiber-optic sensor with colorimetric detection. Anal. Chem. **65:** 331–337.

———, T. R. HAMMAR, S. P. SMITH, AND F. L. SAYLES. 1995a. In situ measurements of seawater pCO_2. Limnol. Oceanogr. **40:** 969–975.

———, W. R. MCGILLIS, N. M. FREW, AND E. J. BOCK. 1995b. Laboratory measurements of seawater CO_2 gas fluxes, p. 375–383. *In* Air-water gas transfer. Select. Pap. 3rd Int. Symp. Aeon.

———, A. VODACEK, R. K. NELSON, E. J. BRUCE, AND N. V. BLOUGH. 1996. Seasonal seawater optical properties of the U.S. Middle Atlantic Bight. J. Geophys. Res. **101:** 22,727–22,736.

DICKEY, T., AND OTHERS. 1993. Seasonal variability of bio-optical and physical properties in the Sargasso Sea. J. Geophys. Res. **98:** 865–898.

FALKOWSKI, P. G., T. S. HOPKINS, AND J. J. WALSH. 1980. An analysis of factors affecting oxygen depletion in the New York Bight. J. Mar. Res. **38:** 479–507.

———, AND OTHERS. 1983. Summer nutrient dynamics in the Middle Atlantic Bight: primary production and utilization of phytoplankton carbon. J. Plankton Res. **5:** 515–537.

FARMER, D. M., C. L. MCNEIL, AND B. D. JOHNSON. 1993. Evidence of the importance of bubbles in increasing air-sea gas flux. Nature **361:** 620–623.

FORSTNER, H., AND E. GNAIGER. 1983. Calculation of equilibrium oxygen concentration, p. 324. *In* E. Gnaiger et al. [eds.], Polarographic oxygen sensors. Springer.

FRIEDERICH, G. E., P. G. BREWER, R. HERLIEN, AND F. P. CHAVEZ. 1995. Measurement of sea surface partial pressure of CO_2 from a moored buoy. Deep-Sea Res. **42:** 1175–1186.

HOPPEMA, J. M. J.. 1991. The seasonal behaviour of carbon dioxide and oxygen in the coastal North Sea along the Netherlands. Neth. J. Sea Res. **28:** 167–179.

JOHNSON, K. M., C. M. BURNEY, AND J. MCN. SIEBURTH. 1981. Enigmatic marine ecosystem metabolism measured by direct diel ΣCO_2 and O_2 flux in conjunction with DOC release and uptake. Mar. Biol. **65:** 49–60.

JOHNSON, K. S., R. M. PYTKOWICZ, AND C. S. WONG. 1979. Biological production and the exchange of oxygen and carbon dioxide across the sea surface in Stuart Channel, British Columbia. Limnol. Oceanogr. **24:** 474–482.

LAWS, E. A. 1991. Photosynthetic quotients, new production and net community production in the open ocean. Deep-Sea Res. **38:** 143–167.

LEWIS, E. R. AND D. W. R. WALLACE. 1995. Basic programs for

the CO_2 system in seawater. Brookhaven Natl. Lab. Publ. BNL-61827.

LISS, P. S., AND L. MERLIVAT. 1986. Air-sea gas exchange rates: Introduction and synthesis, p. 113–129. *In* P. Buat-Menard [ed.], The role of air-sea exchange in geochemical cycling. Reidel.

MCNEIL, C. L., AND D. M. FARMER. 1995. Observations of the influence of diurnal convection on upper ocean dissolved gas measurements. J. Mar. Res. **53:** 151–169.

MILLERO, F. J., AND OTHERS. 1993. The internal consistency of CO_2 measurements in the equatorial Pacific. Mar. Chem. **44:** 269–280.

OUDOT, C. 1989. O_2 and CO_2 balances approach for estimating production in the mixed layer of the tropical Atlantic Ocean (Guinea Dome area). J. Mar. Res. **47:** 385–409.

RICKER, W. E. 1973. Linear regressions in fishery research. J. Fish. Res. Bd. Can. **30:** 409–434.

ROBERTSON, J. E., A. J. WATSON, C. LANGDON, R. D. LING, AND J. W. WOOD. 1993. Diurnal variation in surface pCO_2 and O_2 at 60°N, 20°W in the North Atlantic. Deep-Sea Res. Part 2 **40:** 409–422.

SHARP, J. H., AND T. M. CHURCH. 1981. Biochemical modeling in coastal waters of the Middle Atlantic States. Limnol. Oceanogr. **26:** 843–854.

SIMPSON, J. J. 1985. Air-sea exchange of carbon dioxide and oxygen induced by phytoplankton, methods and interpretation, p. 409–450. *In* Mapping strategies in chemical oceanography. ACS.

TAYLOR, A. H., A. J. WATSON, AND J. E. ROBERTSON. 1992. The influence of the spring phytoplankton bloom on carbon dioxide and oxygen concentrations in the surface waters of the northeast Atlantic during 1989. Deep-Sea Res. **39:** 137–152.

WALLACE, D. W. R. 1994. Anthropogenic chlorofluoromethanes and seasonal mixing rates in the Middle Atlantic Bight. Deep-Sea Res. Part 2 **41:** 307–324.

———, AND C. D. WIRICK. 1992. Large air-sea gas fluxes associated with breaking waves. Nature **356:** 694–696.

WATSON, A. J., C. ROBINSON, J. E. ROBERTSON, P. J. LEB. WILLIAMS, AND M. J. R. FASHAM. 1991. Spatial variability in the sink for atmospheric carbon dioxide in the North Atlantic. Nature **350:** 50–53.

WILLIAMS, P. J. LEB., AND J. E. ROBERTSON. 1991. Overall plankton oxygen and carbon dioxide metabolisms: The problem of reconciling observations and calculations of photosynthetic quotients. J. Plankton Res. **13:** 153–169.